

# HALO FORMATION IN SPHEROIDAL BUNCHES WITH SELF-CONSISTENT STATIONARY DISTRIBUTIONS

A.V. Fedotov, R.L. Gluckstern, University of Maryland, College Park, MD 20742, USA  
S.S. Kurennoy, R.D. Ryne, Los Alamos National Laboratory, Los Alamos, NM 87545, USA

## Abstract

A new class of self-consistent 6-D phase space stationary distributions is constructed both analytically and numerically. The beam is then mismatched longitudinally and/or transversely, and we explore the beam stability and halo formation for the case of 3-D axisymmetric beam bunches using particle-in-cell simulations. We concentrate on beams with bunch length-to-width ratios varying from 1 to 5, which covers the typical range of the APT linac parameters. We find that the longitudinal halo forms first for comparable longitudinal and transverse mismatches. An interesting coupling phenomenon — a longitudinal or transverse halo is observed even for very small mismatches if the mismatch in the other plane is large — is discovered.

## 1 INTRODUCTION

High-intensity applications of ion linacs, such as the transformation of radioactive waste, the tritium production [1], and drivers for spallation neutron sources [2], require peak beam currents up to 100 mA with final energies about 1 GeV and beam losses below 1 ppm. Understanding mechanisms of intense-beam losses, in particular, beam instabilities and halo formation, is of primary importance to satisfy these stringent requirements.

Most efforts in halo formation study have been concentrated so far on 2-D (and often axisymmetric, essentially 1-D) beams, see [3] and references therein. While it produced some analytical results for the simplest case, the K-V distribution, for more realistic distributions particle-core model and particle-in-cell (PIC) simulations have been used, [4]–[10]. As was recognized from these studies, an rms mismatch of the beam to the focusing channel is the main cause of the halo formation.

To single out and explore the mechanism of halo formation associated with the beam rms mismatch, it is important to start from an initial distribution that satisfies the Vlasov-Maxwell equations and, therefore, remains stationary for the matched case. A beam with some initial *non* stationary distribution will evolve from its initial state even being rms-matched to the channel, due to redistribution effects (its evolution is caused by mismatches in higher moments). For 2-D axisymmetric beams, a set of stationary distributions with a sharp beam edge was constructed and explored in [10]:

$$f_n(H) = \begin{cases} N_n n (H_0 - H)^{n-1} & \text{for } H \leq H_0, \\ 0 & \text{for } H > H_0, \end{cases} \quad (1)$$

where  $H$  is the hamiltonian of the transverse motion,  $H_0 = \text{const}$ , and  $N_n$  are normalization constants. The set includes the K-V distribution as a formal limit of  $n \rightarrow 0$ , as well as more realistic ones, like waterbag ( $n = 1$ ) and other distributions, with higher non-linearities in space-charge forces. In this paper, we present results of a similar program in the 3-D case. More details can be found in [11].

## 2 STATIONARY 3-D DISTRIBUTION

### 2.1 Analytical Consideration

We consider a smoothed external focusing with gradients  $k_z, k_y, k_x$ . In general, the beam bunch can be chosen to have an approximately ellipsoidal boundary. For simplicity, we concentrate on the axisymmetric case ( $k_x = k_y$ ), for which the bunch is approximately spheroidal. Our axisymmetric 6-D phase space distribution is

$$f(\mathbf{R}, \mathbf{p}) = N(H_0 - H)^{-1/2}, \quad \text{where} \quad (2)$$

$$H = k_x r^2/2 + k_z z^2/2 + e\Phi_{sc}(\mathbf{R}) + mv^2/2. \quad (3)$$

Here  $\mathbf{p} = m\mathbf{v}$ ,  $r^2 = x^2 + y^2$ , and  $\Phi_{sc}(\mathbf{R})$  is the electrostatic potential due to the space charge. We work in the bunch Lorentz frame, where all motion is non-relativistic.

The distribution (2) is analogous to (1) with  $n = 1/2$ . Since all its dependence on the coordinates is through the hamiltonian  $H = H(\mathbf{R}, \mathbf{p})$ , which is an integral of motion, the distribution is stationary. The same would be true for other exponents in (2); however, for the particular case of  $-1/2$ , the Poisson equation in 3-D case is linear. Namely, it can be written as

$$\nabla^2 G(\mathbf{R}) = -k_s + \kappa^2 G(\mathbf{R}), \quad (4)$$

where  $k_s = 2k_x + k_z$ ,  $\kappa^2 = (eQ/\epsilon_0)/\int d\mathbf{R}G(\mathbf{R})$ ,  $Q$  is the bunch charge, and

$$G(\mathbf{R}) \equiv H_0 - k_x r^2/2 - k_z z^2/2 - e\Phi_{sc}(\mathbf{R}). \quad (5)$$

The solution to Eq. (4) for a spheroidal shaped bunch can be written in the spherical coordinates  $R, \theta$  ( $\cos \theta = z/R$ ,  $\sin \theta = r/R$ ) as  $G(\mathbf{R}) = (k_s/\kappa^2)g(\mathbf{R})$ , where

$$g(\mathbf{R}) = 1 + \sum_{\ell=0}^{\infty} \alpha_{\ell} P_{2\ell}(\cos \theta) i_{2\ell}(\kappa R). \quad (6)$$

Here  $P_{2\ell}(\cos \theta)$  are the even Legendre polynomials and  $i_{2\ell}(\kappa R)$  are the spherical Bessel functions (regular at  $\kappa R =$

0) of imaginary argument. Since  $g(\mathbf{R})$  is proportional to the charge density, the bunch edge is determined by the border  $g(x) = 0$ , closest to the origin. We choose  $\alpha_\ell$ 's to approximate a spheroidal surface with semiaxis  $a$  in the transverse direction and  $c$  in the longitudinal one,  $r^2/a^2 + z^2/c^2 = 1$ .

From the equations of motions, we express the rms tune depressions as

$$\eta_{x,\text{rms}}^2 \equiv \frac{m\langle\dot{x}^2\rangle}{k_x\langle x^2\rangle}, \quad \eta_{z,\text{rms}}^2 \equiv \frac{m\langle\dot{z}^2\rangle}{k_z\langle z^2\rangle}. \quad (7)$$

Note also that  $m\langle\dot{x}^2\rangle = m\langle\dot{y}^2\rangle = m\langle\dot{z}^2\rangle = m\langle v^2\rangle/3$ , because  $H$  depends only on  $v^2$  and  $\mathbf{R}$ . Thus our choice of the form  $f(H)$  automatically corresponds to equipartition (equal average kinetic energy in the three spatial directions). The values of  $\alpha_\ell$  in Eq. (6) for given  $c/a$  and  $\kappa a$  are found by minimizing  $\oint ds g^2(\mathbf{R})$  along the boundary. For a fixed bunch shape  $c/a$ , the rms tune depressions depend on the dimensionless parameter  $\kappa a$  (see in [11]). A contour plot of  $g(\mathbf{R})$  for a typical case  $c/a = 3$ ,  $\kappa a = 3.0$  is shown in Fig. 1. This range of parameters corresponds to the Accelerator Production of Tritium (APT) project [1].

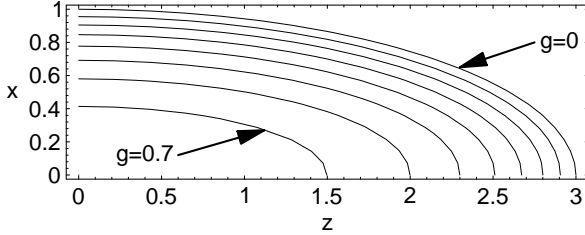


Figure 1: Charge density contours  $g(\mathbf{R}) = \text{const}$  for  $c/a = 3$ ,  $\eta_x = 0.65$ ,  $\eta_z = 0.49$ .

## 2.2 Numerical Investigation

A 3-D particle-in-cell (PIC) code has been developed to test the analytic model of normal modes [11] in the distribution Eq. (2) and to explore halo formation. The single-particle equations of motion are integrated using a symplectic, split-operator technique. The space charge calculation uses area weighting (“Cloud-in-Cell”) and implements open boundary conditions with the Hockney convolution algorithm. The code runs on parallel computers (we mostly used T3E machine at NERSC), and in particular, the space charge calculation has been optimized for parallel platforms. Up to  $2.5 \cdot 10^7$  particles have been used in our simulation runs, with  $10^6$  being a typical number.

Initially, the 6-D phase space is populated according to Eq. (2), and then the  $x, y, z$  coordinates are mismatched by factors  $\mu_x = \mu_y = 1 + \delta a/a$ ,  $\mu_z = 1 + \delta c/c$  and the corresponding momenta by  $1/\mu_x = 1/\mu_y$ ,  $1/\mu_z$ . Simulations show that an initially matched distribution remains stable even for very strong space charge. Introducing some initial mismatch leads to the oscillations of the core, and later on

the beam halo develops, as shown in Fig. 2. This figure shows maximal values  $z_{\text{max}}$  and  $x_{\text{max}}$  of the longitudinal and transverse coordinates (in units of  $a$ ) of the bunch particles versus time, for the case  $\mu_x = \mu_z = \mu$ . The jumps of  $z_{\text{max}}$  and  $x_{\text{max}}$  correspond to the halo formation moments; after that the distribution stabilizes. One can see that the longitudinal halo develops earlier than the transverse one for equal mismatches in both directions. This is in accordance with our expectations since the longitudinal tune depression is lower for an elongated bunch.

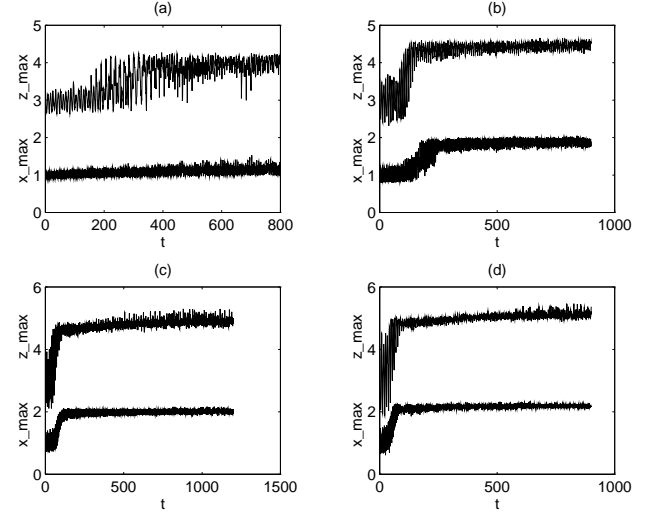


Figure 2: Halo development for increasing mismatches: a)  $\mu = 1.1$ , b)  $\mu = 1.2$ , c)  $\mu = 1.3$ , d)  $\mu = 1.4$ . Time  $t$  is in arbitrary units,  $c/a = 3$ ,  $\eta_x = 0.65$ ,  $\eta_z = 0.49$ .

Choosing larger mismatch either longitudinally or transversely, one can observe primarily the longitudinal or transverse halo, respectively. Results of a systematic study for different bunch shapes  $c/a$  and mismatch parameters are summarized below, first for the longitudinal case.

We define the halo extent as a ratio of the halo maximal size to that of a matched distribution. The **longitudinal halo** extent is found to be approximately linearly proportional to the mismatch. In addition, the ratio  $z_{\text{max}}/(\mu c)$  slightly increases for stronger space charge, from 1.2–1.3 for  $\eta_z$  above 0.5 to 1.4–1.5 for  $\eta_z < 0.4$ . The halo intensity, defined roughly as the fraction of particles outside the bunch core, was also found depending primarily on the mismatch. Large mismatches (40% and higher) lead to several percent of the particles in the halo, which is clearly outside acceptable limits for high-current machines. Obviously, serious efforts should be made to match the beam to the channel as accurately as possible.

For a fixed mismatch, the halo starts to develop earlier for more severe tune depression. Another interesting observation is that for purely longitudinal mismatches ( $\mu_x = 1$ ) in elongated bunches ( $c/a > 2$ ) the longitudinal halo intensity shows a strong dependence on the mismatch. The number of particles in the halo drops dramatically with  $\mu_z > 1$  decreasing; in fact, we see no halo for  $\mu_z < 1.2$ . A similar

threshold behavior was observed in 2-D case [10].

The extent of the **transverse halo** has a similar linear dependence on the mismatch:  $x_{max}/(\mu a)$  depends weakly on  $\eta_x$ , just slightly increasing from 1.4–1.5 for  $\eta_x$  around 0.8 to 1.6–1.8 for  $\eta_x < 0.4$ . Again, the halo intensity is governed primarily by the mismatch. In general, the transverse halo closely duplicates all the features observed for non-linear stationary distributions in 2-D simulations [10]. The only two differences seen are related to the moment and rate of halo development: first, in 3-D simulations it clearly starts earlier for severe tune depression, which was not the case in 2-D; and second, the transverse halo in the 3-D case develops significantly faster than in 2-D for comparable mismatches and tune depressions.

Our 3-D simulations clearly show the **coupling** between the longitudinal and transverse motion: a transverse or longitudinal halo is observed even for a very small mismatch (less than 10%) as long as there is a significant mismatch in the other plane. For example, in Fig. 3 we see a longitudinal halo for only 5% longitudinal mismatch, when  $\mu_x = \mu_y = 1.5$ . The coupling effect is noticeable even for modest mismatches. We mentioned above that  $\mu_z \geq 1.2$  is required to observe a longitudinal halo when  $\mu_x = 1$ . However, when there is a mismatch in all directions, the halo develops even for  $\mu_z = \mu_x = \mu_y = 1.1$  (10% mismatch in all directions). Such a behavior clearly shows the importance of the coupling effect.

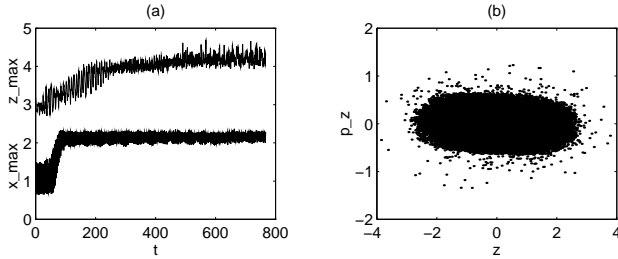


Figure 3: Coupling effect for  $c/a = 3$ ,  $\mu_x = \mu_y = 1.5$ ,  $\mu_z = 1.05$ : (a) maximum  $x$  and  $z$  versus time; (b)  $z$ - $p_z$  phase space diagram (plotted only 32K particles out of  $10^6$  used in simulations).

### 3 SUMMARY AND DISCUSSION

Unlike previous studies of 2-D models of long beams, this paper addresses the beam stability and halo formation in a bunched beam with the parameters in the range of new high-current linac projects [1, 2]. A new class of 6-D phase space stationary distributions for a beam bunch in the shape of a prolate spheroid has been constructed, analytically and numerically. Our choice of parameters automatically assures equipartition. We therefore study the halo development in 3-D bunches which are in thermal equilibrium, without masking effects of the initial-state redistribution. Such an approach allows us to investigate the major mechanism of halo formation associated with the beam mismatch.

Using our PIC code with smoothed linear external focusing forces, by introducing an initial mismatch in the transverse and/or longitudinal directions we find that both transverse and longitudinal halos can develop, depending on the values of tune depressions and mismatches. An interesting new result is that, due to the coupling between the  $r$  and  $z$  planes, a transverse or longitudinal halo is observed for a mismatch less than 10% if the mismatch in the other plane is large. Our main conclusion is that the longitudinal halo is of great importance because it develops earlier than the transverse one for elongated bunches with comparable mismatches in both planes. In addition, its control could be challenging. This conclusion agrees with the results [12] from the particle-core model in spherical bunches.

We expect only small quantitative differences for distributions (2) with other exponents, not  $-1/2$ , based on results for the set (1) in 2-D [10]. More interesting are 3-D effects due to the phase-space redistribution of an initial non-stationary state. Our preliminary results from PIC simulations show that the redistribution process can produce the beam halo in the same fashion as a small rms mismatch [13]. A similar conclusion was made for 2-D axisymmetric beams [5, 9]. In 3-D, however, the effect can be amplified by the coupling, especially noticeable in the bunches with  $c/a$  close to 1.

The authors would like to acknowledge support from the U.S. Department of Energy, and to thank R.A. Jameson and T.P. Wangler for useful discussions.

### 4 REFERENCES

- [1] APT Conceptual Design Report, LA-UR-97-1329, Los Alamos, NM, 1997.
- [2] SNS Conceptual Design Report, NSNS-CDR-2/V1, Oak Ridge, TN, 1997.
- [3] M. Reiser, Theory and Design of Charged Particle Beams, Wiley, New York (1994).
- [4] R.L. Gluckstern, Phys. Rev. Lett. **73**, 1247 (1994).
- [5] R.A. Jameson, in 'Frontiers of Accelerator Technology', World Scient., Singapore, 1996, p. 530.
- [6] S.Y. Lee and A. Riabko, Phys. Rev. E **51**, 1609 (1995).
- [7] T.P. Wangler, et al, in Proceed. of LINAC96, Geneva, Switzerland (1996). - CERN 96-07, p.372.
- [8] R.L. Gluckstern, W-H. Cheng, S.S. Kurennoy and H. Ye, Phys. Rev. E **54**, 6788 (1996).
- [9] H. Okamoto and M. Ikegami, Phys. Rev. E **55**, 4694 (1997).
- [10] R.L. Gluckstern and S.S. Kurennoy, in Proceed. of PAC97, Vancouver, BC, Canada (1997).
- [11] R.L. Gluckstern, A.V. Fedotov, S.S. Kurennoy and R.D. Ryne, Univ. of Maryland, Phys. Dept. preprint 98-107, College Park, MD, 1998; submitted to Phys. Rev. E.
- [12] J.J. Barnard and S.M. Lund, I & II, in Proceed. of PAC97, Vancouver, BC, Canada (1997).
- [13] A.V. Fedotov, R.L. Gluckstern, S.S. Kurennoy and R.D. Ryne, Univ. of Maryland, Phys. Dept. preprint 98-108, College Park, MD, 1998; to be published.